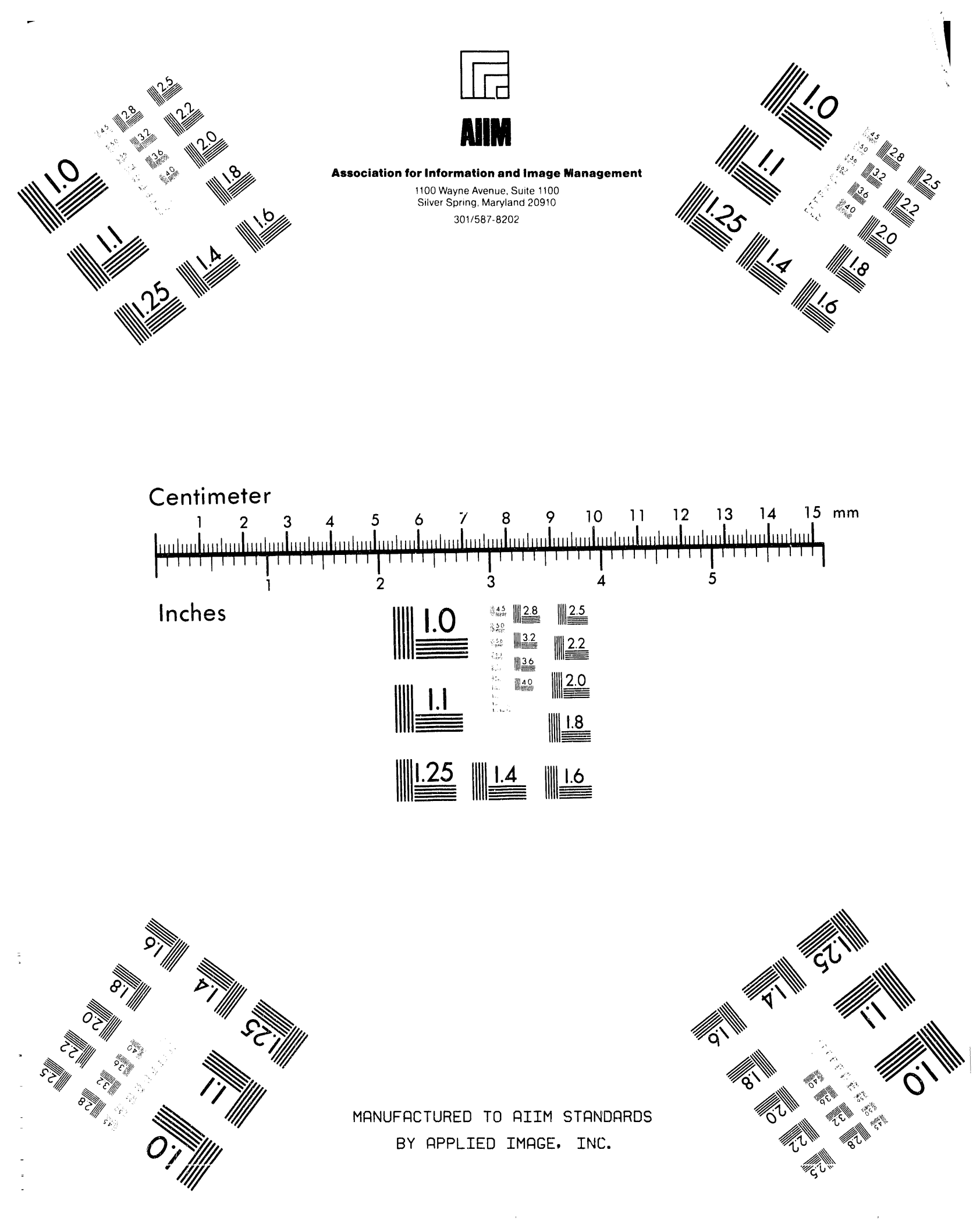
AIIM
Association for Information and Image Management
1100 Wayne Avenue, Suite 1100
Silver Spring, Maryland 20910
301/587-8202
Centimeter
Inches
MANUFACTURED TO AIIM STANDARDS
BY APPLIED IMAGE, INC.

1 of 1

LBL-30117

Grid Orientation Effects in the Simulation of Cold Water Injection into Depleted Vapor Zones

K. Pruess

Earth Sciences Division
Lawrence Berkeley Laboratory
University of California
Berkeley, California 94720

January 1991

This work was supported by the Assistant Secretary for Conservation and Renewable Energy, Office of Renewable Technologies, Geothermal Technology Division, of the U.S. Department of Energy under Contract No. DE-AC03-76SF00098.

Grid Orientation Effects in the Simulation of Cold Water Injection into Depleted Vapor Zones

Karsten Pruess

Earth Sciences Division, Lawrence Berkeley Laboratory
University of California, Berkeley, CA 94720

Introduction

Vapor-dominated geothermal reservoirs such as Larderello, Italy, and The Geysers, California, are fundamentally water-short systems. This is apparent from the relatively low pressures in the natural state, typically about 35 bars at 1000 m depth, which is much below hydrostatic pressures. It is also apparent from the high heat content of the produced fluids, typically superheated steam.

Large-scale production from these systems has caused reservoir pressures and well flow rates to decline, leading to an underutilization of installed electrical generating capacity. Clearly, these reservoirs are beginning to run out of fluid, while heat reserves in place are still enormous. (At Larderello, there is a long-term trend of increasing formation temperatures in the upper productive zones of the reservoir; Sestini, 1970). Reinjection of colder waste waters, or injection of waters from a source other than the geothermal reservoir, is the primary means by which dwindling fluid reserves can be replenished.

A considerable body of field experience with injection has been accumulated at Larderello and The Geysers; the results have been mixed. There are well documented cases where injection has increased flow rates of nearby wells. Return of injected fluid as steam from production wells has been observed directly through chemical and isotopic changes of produced fluids (Giovannoni et al., 1981; Nuti et al., 1981). In other cases injection has caused thermal interference and has degraded the temperature and pressure of production wells.

Water injection *into* depleted vapor zones gives rise to complex two-phase fluid flow and heat transfer processes with phase change. These are further complicated by the fractured-porous nature of the reservoir rocks. An optimization of injection design and operating practice is desirable; this requires realistic and robust mathematical modeling capabilities.

Numerical Simulation of Water Injection

Water injection into a medium containing superheated vapor can be classified as a process of immiscible displacement, which is made considerably more complicated by the fact that some of the displacing water may vaporize, while some of the vapor undergoing displacement may condense. These phase change processes are accompanied by strong latent heat effects. The large contrast in thermophysical properties between water and vapor (see Table 1) gives rise to highly non-linear flow behavior.

A number of papers have presented numerical simulations of cold water injection into superheated vapor zones (O'Sullivan and Pruess, 1980; Schroeder et al., 1982; Calore et al., 1986; Pruess et al., 1987). These studies have demonstrated numerical simulation techniques that are capable of dealing with the highly non-linear processes, and have clarified some of the basic effects and phenomena. Flow around an injection well has been analyzed under the simplifying assumptions of horizontal flow only, and radial symmetry. Around the injection well, a single-phase liquid plume forms with a temperature equal to the injection temperature $T = T_{inj}$ (see Figure 1). Beyond this plume there is a region of single-phase liquid conditions, with temperature $T = T_f$ intermediate between injection temperature and original reservoir temperature T_o, $T_{inj} < T_f < T_o$. In a porous medium, and neglecting the (small) effects of heat conduction, the temperature and phase fronts are sharp. Heat conduction broadens the fronts slightly, while in fractured-porous media the delayed fluid flow and heat transfer between fractures and rock matrix can lead to very broad temperature fronts and extended two-phase zones containing a ''ing mixture of water and vapor (Calore et al., 198[illegible]

Injection effects are much more complicated when the possibility of vertical flow is taken into consideration (Calore et al., 1986). Vertical permeability permits injected water to flow downward in addition to outward. Because of the much larger density of liquid water as compared to vapor, downward flow of liquid does not require a pressure gradient, but can be driven by gravity force, even opposing a (sub-hydrostatic) gradient. The effect of gravity may dominate the pressure and temperature regime around an injection well. Much of the injected water may flow downward rather than outward from the injection well, partially vaporizing in the pro-

cess. Two-phase conditions may extend all the way to the injection well. The one-to-one correspondence between pressure and temperature in two-phase conditions can give rise to interesting heat pipe effects (water-vapor counterflow; Calore et al., 1986). Over time, temperatures near the injection well will decline. As long as two-phase conditions prevail, this will be accompanied by pressure decline, so that within the boiling injection plume vapor will flow towards the injection well rather than away from it. Vapor approaching the injection point will partially condense, and the associated latent heat effects will counter the cooling effects from continued injection. The entire injection plume may remain in boiling and nearly isothermal conditions, maintained by water-vapor counterflow (heat pipe). When the injection rate is increased, pressures near the injection well will also increase, and a single-phase liquid zone of limited extent may form. Temperatures in the liquid zone will decline towards the injection temperature. The flow processes are further complicated by preferential flow in fractures, and by the unstable nature of a displacement process in which a heavier phase (water) is invading a region with lighter fluid (vapor) from above.

Numerical simulation studies have shown that predictions of water injection into vapor zones are sensitive to space and time discretization effects. Space discretization effects are well known from immiscible displacement processes, where they cause a broadening of phase fronts (Aziz and Settari, 1977). These effects are aggravated in two-phase flow with phase change, because they affect the coupling between fluid flow and heat transfer, and alter the phase composition of the flowing two-phase mixture. Coarse gridding near the injection point will cause an over-prediction of vaporization rates. The one-to-one correspondence between temperatures and pressures in two-phase conditions can produce spurious flow effects (Schroeder et al., 1982; Pruess et al., 1987): when colder water enters a grid block that is in two-phase conditions, temperature and pressure of the two-phase mixture decline, causing spurious flow towards the injection point. In simulations of cold water injection into superheated vapor zones in two-dimensional R-Z geometry, the shape of the injection plume was found to depend sensitively on the computational grid used (unpublished work by the author with R. Celati and C. Calore).

Because of the sensitivity to space discretization effects, there is lingering concern about the realism and credibility of numerical simulation predictions for injection into superheated vapor zones. The present paper focusses on a particular kind of space discretization effects, associated not with the size of computational grid blocks but with the orientation of the grid lines. The basic mass and energy balance equations applicable for the process of water injection into isotropic media are rotationally invariant in the horizontal plane, while a computational grid introduces preferred directions. For example, a conventional finite-difference grid consisting of identical squares permits flow to or from a grid block only in discrete directions of 0°, 90°, 180°, and 270°. This discreteness in the rotational sense persists even as grid spacing is refined, causing grid orientation errors.

A potential for grid orientation errors exists also in the vertical plane, where the vector of gravitational acceleration defines a preferred direction. Simulation predictions may be sensitive to the orientation of grid lines with respect to the vertical.

Studies of two-phase immiscible displacement, and of steam flooding of hydrocarbon reservoirs, have shown that mere grid refinement is ineffective in reducing grid orientation errors. Such errors can be substantially eliminated only by increasing the number of flow directions considered in the finite difference grid. Conventional finite difference simulations employ a "five-point" differencing scheme, which considers flow between a grid cell and the four neighbors with which it shares interfaces (see Figure 2; P communicating with E, N, W, and S). Grid orientation effects can be substantially reduced by means of a "nine-point" approximation, which in addition considers the possibility of flow along the diagonal directions (P communicating with NE, NW, SW, and SE).

This paper examines grid orientation effects for simulation of water injection into depleted (low pressure) vapor zones. We study grid orientation effects not only in the horizontal plane, but also in the vertical direction. All simulations were carried out with LBL's general-purpose reservoir simulator TOUGH2 (Pruess, 1990), which implements the general MULKOM architecture for multiphase fluid and heat flows (Pruess, 1983, 1988).

2-D Areal Model

The nature and strength of grid orientation effects can be easily evaluated by comparing simulation results obtained from two different grids that have the same grid block size but different orientation. The customary approach is to consider a five-spot production-injection arrangement, and to compare simulations obtained with "parallel" and "diagonal" grids (see Figure 3; the terms "parallel" and "diagonal" denote the direction of grid lines relative to the lines connecting production and injection wells). We have performed simulations with the grids shown in Figure 3, using problem parameters applicable for depleted vapor zones at Larderello or The Geysers (see Table 2). Results for production rates and temperatures predicted from the two different grids are given in Table 3.

It is apparent that the predictions from both grids are very similar. Early on, there is slightly faster water migration towards the production well in the parallel grid, giving somewhat higher production rates and slightly faster cooling near the production well. In the middle period, 5 - 10 years, predictions from both grids are in excellent agreement, while subsequently there again is somewhat more cooling along the flowpath from

the injector to the producer in the parallel grid. Additional simulations were performed with a "two-waters" description of the process, where injected water can be distinguished from the vapor originally in place, so that the mixture of injected and in-place fluid extracted at the production well can be monitored. The parallel grid predicted a more rapid initial return of vaporized injected water than the diagonal grid. However, these differences persist for only a very brief period (a few weeks) after start of injection.

In summary, we conclude that grid orientation effects for simulation of water injection into low-pressure vapor zones are insignificant in 2-D areal models. This favorable result can be understood in terms of the "favorable mobility ratio" between injected and displaced fluid. When water displaces vapor, the displacing fluid has higher viscosity and poses greater resistance to flow. The parallel grid tends to facilitate migration from the injector to the producer; however, as more of the flow path towards the production well fills with liquid water, flow resistance increases, diminishing the preferential flow. An analogous process will take place in the diagonal grid. In this case, initial water flow will preferentially occur in the diagonal direction. As water saturation in this direction increases, the viscosity contrast will then diminish diagonal flow. In this fashion, a displacement with favorable mobility ratio will tend to reduce differences in numerical simulation predictions from grids with different orientations of grid lines.

Water injection into superheated vapor zones has characteristics opposite from those encountered in steam flooding of hydrocarbon reservoirs, an "unfavorable mobility ratio" displacement. In the latter process, the viscosity of the displacing fluids (steam and oil heated to high temperature) will be much less than the viscosity of the displaced fluids (water and oil at ambient temperature). Therefore, flow resistance along the path of displacing fluids will diminish, so that any preferential displacement in a particular direction will tend to get amplified, giving rise to very strong grid orientation effects (Coats and Ramesh, 1982).

2-D Vertical Section

The areal simulations discussed in the previous section may not give a realistic outlook on effects of water injection into low-pressure vapor zones. Liquid water is much heavier than steam and may flow preferentially downward from an injection point rather than outward. Injection of heavier fluid into lighter fluid from above is subject to gravitational instabilities (Schubert and Straus, 1980), which suggests a potential for strong grid orientation effects in the vertical direction.

To examine this possibility, we have performed simulations of water injection into vertical-section models, using parallel as well as diagonal grids. From a practical viewpoint, the main interest is in the effects of the injection plume on conditions in the surrounding reservoir. Volume, shape, and thermodynamic conditions of the plume must be modeled accurately so that the rate at which the boiling plume supplies vapor to the reservoir may be predicted. In the vicinity of an injection well, flow geometry is cylindrically symmetric, requiring a two-dimensional axisymmetric (R-Z) grid. However, in our studies we have employed two-dimensional linear vertical section (X-Z) grids, for the following reason. It is well established that grid orientation effects can often be alleviated by means of higher-order differencing methods, such as nine-point differencing. Our choice of an X-Z section was made because implementation of higher-order differencing is straightforward for grids of constant thickness. R-Z grids would pose added complications, because the volumes of grid blocks with constant vertical cross-sectional area increase with distance from the symmetry axis.

The model system chosen for simulation of water injection is shown in Figure 4. It has a vertical extent of 200 m, a thickness of 1 m, and a horizontal length of approximately 200 m (slightly different for the parallel and diagonal grids; see below). Injection is made at the top of the left vertical boundary, while at the right vertical boundary constant pressures corresponding to gravity equilibrium are maintained. The gravity equilibrium is obtained by first running initial conditions of T = 240°C and P = 10 bar to steady state. Problem parameters are given in Table 2.

Schematic diagrams of parallel and diagonal grids are shown in Figure 5. The parallel grid used in most simulations has a block size of $\Delta x = \Delta z = 10$ m. However, the left vertical boundary, where injection is made, is interpreted as a symmetry boundary, so that the first Δx is 5 m, and the first column of nodal points is located right on the boundary. For the diagonal grid we wish to employ grid blocks of approximately the same volume. The length of the diagonal in the parallel grid is $\sqrt{200}$ = 14.14 m. In order to cover the same vertical distance of 200 m in the diagonal grid, we take the length of the diagonal in the diagonal grid as 200/14 = 14.29 m, to which corresponds a side length of 10.10 m. Thus, the blocks in the diagonal grid have very nearly the same volume as those in the parallel grid. The parallel grid has 20 rows by 21 columns, and a total volume of 41,000 m^3, as compared to the diagonal grid which has 29 rows by 30 columns, with a volume of 42,142.8 m^3.

Results of simulations are presented as contour diagrams of injection plumes (region of two-phase or single-phase liquid conditions) after 717.01 days of simulated time (Figures 6 through 9), and as a table of fractions of injected water vaporized (Table 4). The plume diagrams provide a detailed picture of injection behavior, while the vaporization fractions give a broad aggregate measure.

Results for Five-Point Parallel and Diagonal Grids

Figure 6 compares the injection plumes after 717.01 days of simulated time with the parallel and diagonal grids, respectively. The discrepancies are very large indeed. In the parallel grid, all flow is vertically downward from the injection point. The vaporizing liquid flows towards the bottom of the flow system, and is then diverted laterally outward. There is no lateral component to liquid phase flow above the bottom row of grid blocks. The diagonal grid on the other hand predicts a plume of considerable lateral extent, approximately 50 m, with only a small amount of accumulation of two-phase fluid at the bottom. This comparison shows that grid orientation effects in the vertical can be extremely strong for water injection into low-pressure vapor zones. For comparison, another simulation was performed with the parallel grid, in which the regions of the plume were more finely discretized. The first (leftmost) column of grid blocks (Δx = 5 m) was further partitioned into three columns of Δx = 1 m, 2 m, 2 m, and the last (bottom-most) row with Δz = 10 m was partitioned into four rows of Δz = 5 m, 2 m, 2 m, and 1 m. The results were very similar to those of the coarser parallel mesh, indicating that the grid orientation errors are not overcome by finer discretization. We emphasize in passing the seriousness of grid size errors. Heat balance considerations show that complete vaporization of the injected water would cool a reservoir volume of 1 m^3 by 1.177 10^{-2} °C per second. If the entire "parallel grid" flow system of 41,000 m^3 volume would be represented with one grid block, total vaporization would effect a cooling by 17.78 °C over the 717.01 days injection period. In such a coarse grid the temperature would therefore remain above the saturation temperature at prevailing pressures of approximately 10 bars; all the injectate would be completely vaporized, and no injection plume would form.

Results for Nine-Point Differencing

After demonstration of extremely strong grid orientation effects in the vertical, the next set of simulations was carried out with the objective to determine whether these effects could be substantially eliminated by means of a differencing scheme with a higher order of rotational accuracy. Figure 7 compares predicted injection plumes after 717.01 days of simulated time for parallel and diagonal 9-point grids. The predictions for the shape of the injection plumes are similar, indicating that grid orientation effects have been much reduced. However, some significant differences persist. The diagonal 9-point simulation predicts significantly more water migration near the bottom of the reservoir. The plume predicted from the 9-point parallel grid detaches from the injection boundary about halfway down. Additional minor differences exist with respect to the phase distribution within the plume. Predictions for vaporization fractions, providing an integrated view of injection effects, agree well between the parallel and diagonal 9-point grids (Table 4).

It can be concluded that 9-point differencing cures much of the grid orientation problem, but significant grid orientation errors persist. This is not surprising in view of the fact that 9-point differencing is designed to preserve the rotational invariance of the Laplace operator to higher order (Forsythe and Wasow, 1960). This is the dominant term in pressure-driven displacement in the horizontal plane; however, the vertical flow in the present injection problem arises from the gravity term in Darcy's law, which contributes a first-order spatial derivative term in the governing equations. Improving on the finite-difference approximation of the Laplacian would not necessarily improve the discretized representation of the gravity flow term.

The problem considered so far - cold water injection into a porous medium containing superheated steam, subject to pressure and gravity forces, and heat exchange with phase transformation effects - is highly idealized. It simplifies the "real" problem by neglecting several physical effects, including capillary pressures, hydrodynamic dispersion, vapor pressure lowering, and formation heterogeneity (fractured-porous medium). While simplifying the physics, these idealizations actually make the problem more difficult and sensitive from the viewpoint of numerical simulation. The idealized problem considered so far is highly hyperbolic in nature, while incorporation of more realistic physical effects would make the problem more diffusive, or parabolic, and less subject to numerical discretization errors. For example, capillary pressure effects would tend to suck injected water into dryer regions, giving rise to horizontal flow of water away from the injection point.

Capillary Pressure Effects

Simulations incorporating capillary pressure effects were carried out to examine whether inclusion of such effects would significantly improve grid orientation performance. We have no data for capillary pressure functions applicable to the Larderello or Geysers systems, and have rather arbitrarily chosen the following functional form (Leverett, 1941; Udell and Fitch, 1985):

$$P_{cap} = -40 \cdot 10^6 \cdot \sigma \cdot f(S_l) \qquad (1)$$

where $f = 1.417\ (1-S_l) - 2.120\ (1-S_l)^2 + 1.263\ (1-S_l)^3$ is a function of liquid saturation S_l, and σ is the surface tension of water, a function of temperature.

Results of injection simulations with parallel and diagonal 9-point grids, incorporating capillary pressure effects, are shown in Figure 8. There is close agreement between the two predictions for the injection plume, indicating that grid orientation effects have been substantially eliminated. In addition to helping reduce grid orientation effects, inclusion of capillary forces has also eliminated the slumping of injected water to the reservoir bottom, and it has effected a certain lateral broadening of the plume. Predicted vaporization fractions from

parallel and diagonal grids show excellent agreement at all times (Table 4).

For completeness, we also present results of simulations with capillary pressure effects in 5-point parallel and diagonal grids (Figure 9). The discrepancies between the two grids are not very large, but considerably stronger than for 9-point differencing. Agreement between the predicted vaporization fractions is good (Table 4). For the diagonal grid, predictions from the 5- and 9-point schemes are very similar, while for the parallel grid the discrepancies are larger.

Discussion and Conclusions

The goal of numerically simulating injection is to provide a robust and realistic prediction of injection effects. Presently available numerical simulators can successfully model the basic physical processes associated with injection of cold water into superheated vapor zones, including highly non-linear phase transitions from vapor to two-phase to liquid conditions, and the associated strongly coupled fluid flow and heat transfer effects. However, this capability for simulating the basic processes does not necessarily guarantee realistic predictions for practical injection problems that involve multidimensional flow effects on a broad range of space and time scales.

Ideally, numerical simulation predictions should be independent of the orientation of the computational grid used. However, our studies showed a potential for very strong grid orientation errors, and determined remedies to alleviate them. Specific results for the parameters and conditions investigated in this study are as follows.

(1) Grid orientation effects in the horizontal plane are insignificant, as would be expected from the favorable mobility ratio between liquid and vapor phases (more viscous water displacing less viscous vapor).

(2) Grid orientation effects in the vertical direction can be exceedingly strong. The most commonly used rectangular grids with vertical grid lines may give totally erroneous results. These grid orientation errors are not diminished by finer space discretization.

The following observations pertain to grid orientation effects in the vertical plane.

(3) Diagonal grids (grid lines oriented at 45° to the vertical) perform rather well, yielding results free of obvious large errors.

(4) Higher-order differencing (9-point versus the conventional 5-point) significantly reduces grid orientation errors. Results for parallel and diagonal grids are in approximate agreement when 9-point differencing is used.

(5) The pathological features observed for 5-point differencing in parallel grids disappear when capillary pressure effects are taken into account. Inclusion of capillary pressures makes for a more realistic process description (obviously, appropriate capillary pressure data are required), and it simplifies the attainment of simulation results that are free of large errors.

Simulations including capillary pressure effects with parallel and diagonal grids are in approximate agreement and give generally acceptable results. The best results are obtained when 9-point differencing is used, but the improvements in numerical performance obtained by including capillary pressure effects are more significant than the improvements resulting from higher-order differencing. Capillary pressures combat the fingering associated with the gravitational instability of heavier fluid (water) over lighter fluid (vapor). Hydrodynamic dispersion, which has not been explicitly modeled in the present work, will have similar effects. The better performance of the diagonal grid, even when only 5-point differencing is used, may be interpreted as resulting from an artificial (numerical) dispersion perpendicular to the (vertical) direction of unstable gravitational fingering. Hydrodynamic dispersion effects are expected to be quite significant in fractured reservoirs, such as Larderello and The Geysers, and deserve further study. Future work should also address the special effects from the radially divergent (as opposed to linear) flow geometry around an injection well.

Acknowledgement

The author would like to thank Michael O'Sullivan for reviewing the manuscript and suggesting improvements. This work was supported by the Geothermal Technology Division, U. S. Department of Energy, under Contract No. DE-AC03-76SF00098. The numerical computations were performed at the National Energy Research Supercomputer Center, with support from the Office of Basic Energy Sciences, U. S. Department of Energy.

References

Calore, C., Pruess, K., and Celati, R., (1986). Modeling Studies of Cold Water Injection into Fluid-Depleted, Vapor-Dominated Geothermal Reservoirs, paper presented at the Eleventh Workshop Geothermal Reservoir Engineering, Stanford University, Stanford, Ca.

Coats, K. H., and Ramesh, A. B., (1982). Effects of Grid Type and Difference Scheme on Pattern Steamflood Simulation Results, paper SPE-11079, presented at the 57th Annual Fall Technical Conference and Exhibition of the Society of Petroleum Engineers, New Orleans, La.

Forsythe, G. E. and Wasow, W. R., (1960). *Finite-Difference Methods for Partial Differential Equations*, John Wiley and Sons, Inc., New York, London.

Giovannoni, A., Allegrini, G., Cappetti, G., and Celati, R. (1981). First Results of a Reinjection Experiment at

Larderello, Proceedings, Seventh Workshop Geothermal Reservoir Engineering, Stanford University, SGP-TR-55.

Leverett, M. C., (1941). Capillary Behavior in Porous Solids, *AIME Trans., 142,* 152.

Nuti, S., Calore, C. and Noto, P., (1981). Use of Environmental Isotopes as Natural Tracers in a Reinjection Experiment at Larderello, Proceedings, Seventh Workshop Geothermal Reservoir Engineering, Stanford University, SGP-TR-55.

O'Sullivan, M. J. and Pruess, K., (1980). Numerical Studies of the Energy Sweep in Five-Spot Geothermal Production/Injection Systems, Proceedings, Sixth Workshop Geothermal Reservoir Engineering, Stanford University, SGP-TR-50.

Schroeder, R. C., O'Sullivan, M. J., Pruess, K., Celati, R. and Ruffilli, C., (1982). Reinjection Studies of Vapor-Dominated Systems, *Geothermics, 11,* (2), 93-120.

Pruess K., (1983). Development of the General Purpose Simulator MULKOM, Annual Report 1982, Earth Sciences Division, Lawrence Berkeley Laboratory LBL-1550.

Pruess, K., (1988). SHAFT, MULKOM, TOUGH: A Set of Numerical Simulators for Multiphase Fluid and Heat Flow, *Geotermia, Rev. Mex. Geoenergia, 4,* (1) 185-202.

Pruess, K., (1990). TOUGH2 - A General-Purpose Numerical Simulator for Multiphase Fluid and Heat Flow, Lawrence Berkeley Laboratory Report LBL-29400.

Pruess, K. and Bodvarsson, G. S., (1983). A Seven-Point Finite Difference Method for Improved Grid Orientation Performance in Pattern Steam Floods, paper SPE-12252, presented at the Seventh Society of Petroleum Engineers Symposium on Reservoir Simulation, San Francisco.

Pruess, K., Calore, C., Celati, R. and Wu, Y. S., (1987). An Analytical Solution for Heat Transfer at a Boiling Front Moving through a Porous Medium, *Int. J. of Heat and Mass Transfer, 30,* (12) 2595-2602.

Schubert, G. and Straus, J. M., (1980). Gravitational Stability of Water over Steam in Vapor-Dominated Geothermal Systems, *J. Geophys. Res., 85,* 6505-6512.

Sestini, G., (1970). Superheating of Geothermal Steam, *Geothermics,* Special Issue 2, 622-648.

Udell, K. S. and Fitch, J. S., (1985). Heat and Mass Transfer in Capillary Porous Media Considering Evaporation, Condensation, and Non-condensible Gas Effects, paper presented at 23rd ASME/AIChE National Heat Transfer Conference, Denver, CO.

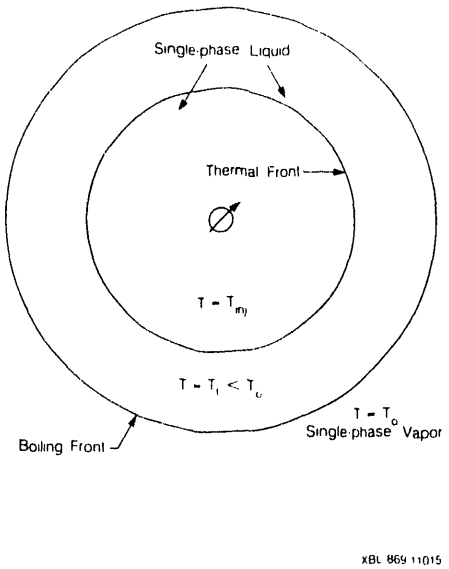

Figure 1. Schematic diagram of fronts for cold water injection into a super-heated vapor zone in 1-D radial flow approximation (from Pruess et al., 1987).

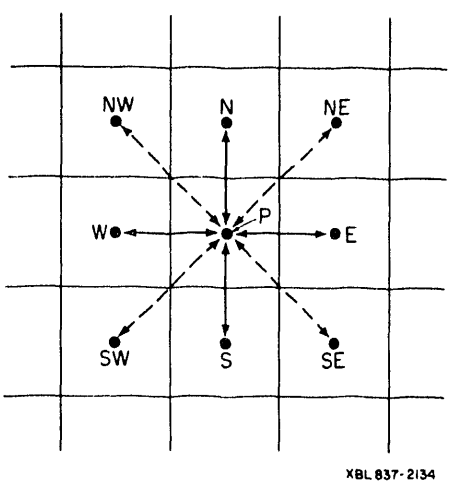

Figure 2. Five- and nine-point finite difference approximations (from Pruess and Bodvarsson, 1983).

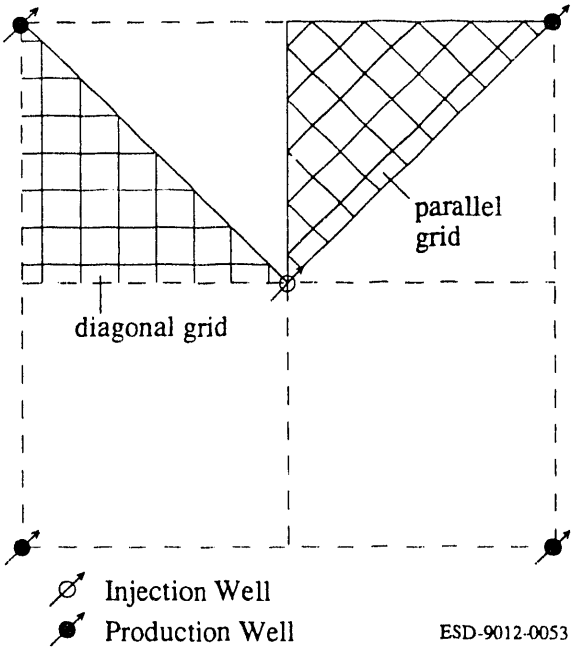

Figure 3. Five-spot well pattern with parallel and diagonal grids for modeling a 1/8 symmetry domain.

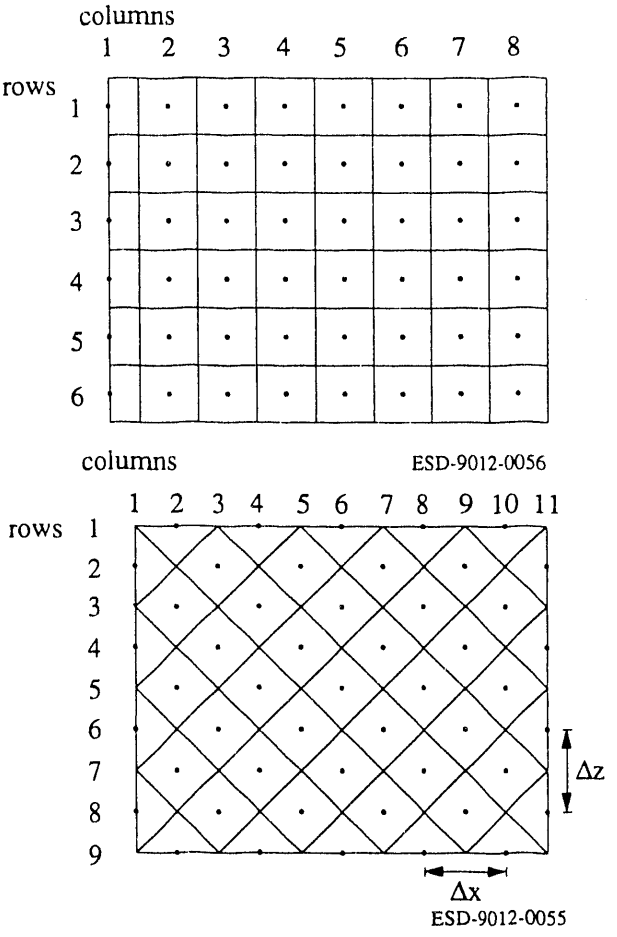

Figure 5. Schematic of parallel and diagonal grids used for modeling injection in 2-D vertical section.

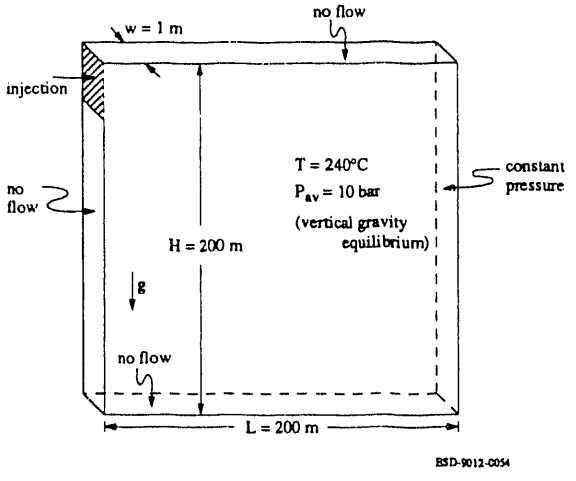

Figure 4. Schematic of 2-D vertical section.

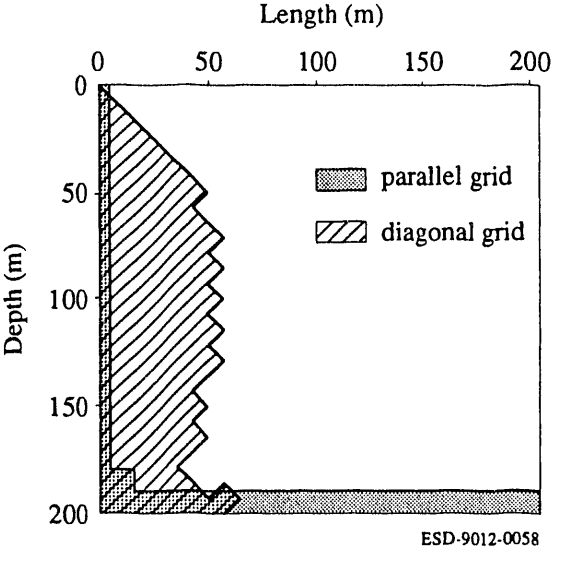

Figure 6. Simulated plumes after 717.01 days of injection in parallel and diagonal 5-point grids.

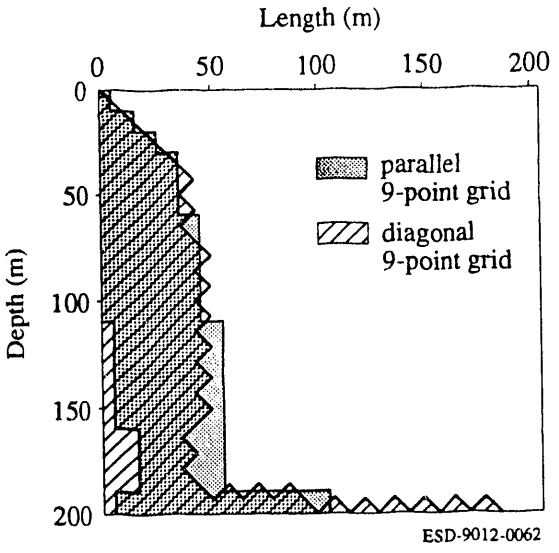

Figure 7. Simulated injection plumes after 717.01 days for 9-point differencing.

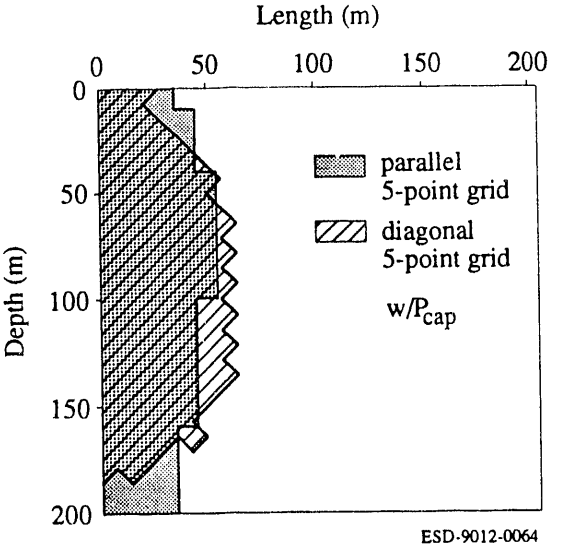

Figure 9. Simulated injection plumes after 717.01 days with capillary pressure effects included; 5-point differencing.

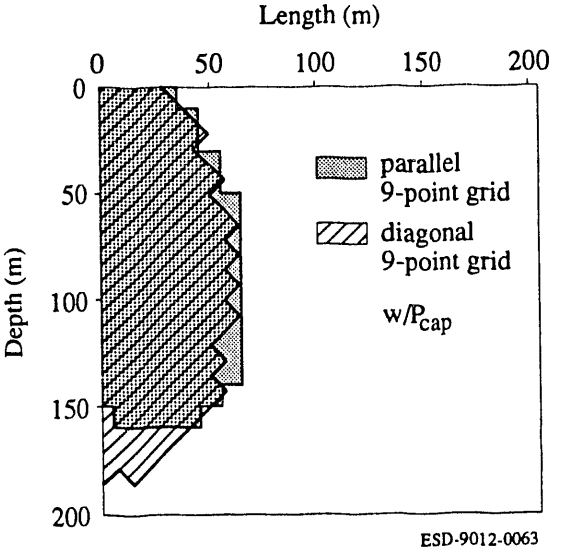

Figure 8. Simulated injection plumes after 717.01 days with capillary pressure effects included; 9-point differencing.

Table 1. Selected thermophysical properties of water and vapor at saturated conditions of 240°C.

	Density (kg/m^3)	Enthalpy (kJ/kg)	Viscosity (Pa·s)
Water	813.7	1037.3	$1.11 \cdot 10^{-4}$
Vapor	16.7	2803.8	$0.17 \cdot 10^{-4}$

Table 2. Parameters used in simulations.

Formation Parameters	
rock density	2600 kg/m^3
porosity	0.05
thermal conductivity	2.51 W/m°C
specific heat	920 J/kg°C
permeability	(a) $1 \cdot 10^{-13}$ m^2 (b) $1 \cdot 10^{-12}$ m^2
relative permeability	Corey curves with Slr = 0.30 Sgr = 0.05
capillary pressure	0, or Leverett J-function (see text)
Initial Conditions	
temperature	240°C
pressure	(a) 10 bar (b) gravity equilibrium with P_{av} = 10 bar
Injection Specifications	
enthalpy	126 kJ/kg (approximately 30°C)
injection rate	(a) 2.5 kg/s (b) 0.01 kg/s
Production Specifications	
(a) wellbore pressure	8 bar
(a) productivity index	$8.335 \cdot 10^{-12}$ m^3
(b) Variable rate at constant pressure boundary	

(a) 1/8 of five-spot with 208.5 m well spacing (20 acre), 200 m thick
(b) vertical X-Z section with depth = 200 m, thickness = 1 m

Table 3. Simulated production rates and temperatures for five-spot areal production-injection system, using parallel and diagonal grids.

Time (years)	Production Rate (kg/s)		Production Temperature (°C)	
	parallel	diagonal	parallel	diagonal
2	1.60	1.28	226.5	233.5
5	2.18	2.40	192.3	190.6
10	2.41	2.44	185.5	186.5
20	2.48	2.48	157.6	163.0

Table 4. Fraction of injected water vaporized for 2-D vertical section.

Time (days)	Grid	5-point		9-point	
		no P_{cap}	w/P_{cap}	no P_{cap}	w/P_{cap}
37.0	parallel	0.707	0.774	0.700	0.761
	diagonal	0.696	0.750	0.717	0.765
105.3	parallel	0.747	0.725	0.729	0.736
	diagonal	0.720	0.714	0.721	0.743
214.1	parallel	0.703	0.702	0.729	0.730
	diagonal	0.714	0.711	0.720	0.712
329.9	parallel	0.677	0.722	0.715	0.712
	diagonal	0.705	0.713	0.706	0.715
501.1	parallel	0.756 (*)	0.709	0.715	0.707
	diagonal	0.710	0.715	0.708	0.715
614.6	parallel	0.800 (*)	0.719	0.701	0.713
	diagonal	0.716	0.715	0.695	0.713
717.0	parallel	0.828 (*)	0.715	0.686	0.708
	diagonal	0.689	0.716	0.677	0.715

(*) Injection plume has penetrated constant-pressure boundary.

DATE
FILMED
8/31/93
END